11 Autocorrelations in Quantum Monte Carlo Simulations of Electron-Phonon Models

Martin Hohenadler[1] and Thomas C. Lang[2]

[1] Theory of Condensed Matter, Cavendish Laboratory, University of Cambridge, Cambridge CB3 0HE, United Kingdom
[2] Institut für Theoretische Physik und Astrophysik, Universität Würzburg, 97074 Würzburg, Germany

The problem of autocorrelations in quantum Monte Carlo simulations of electron-phonon models is analysed for different algorithms in the framework of the Holstein model. By revisiting several cases found in the literature, it is demonstrated that neglecting autocorrelations can lead to an underestimation of statistical errors by orders of magnitude and hence to incorrect results. A modified algorithm for certain Holstein-type models, free of any autocorrelations, is discussed.

11.1 Introduction

The interaction of electrons with lattice degrees of freedom plays an important role in many materials, including conventional and high-temperature superconductors, colossal-magnetoresistance manganites, and low-dimensional nanostructures. Over more than two decades, lattice and continuum quantum Monte Carlo (QMC) simulations have proved to be a highly valuable tool to investigate the properties of coupled fermion-boson models in condensed matter theory.

Despite the recent development of other numerical methods (e.g., the density matrix renormalization group, see Part IX, QMC approaches remain in the focus of research due to their versatility. Especially in the early days of computational physics, they outperformed alternative memory-consumptive methods, and this often remains true today, e.g., in more than one dimension or at finite temperature. Apart from stand-alone applications, QMC algorithms also serve as solvers in the context of cluster methods (see Chap. 16). Finally, they represent the most reliable techniques for several classes of problems, e.g., three-dimensional (3D) spin systems (see Chap. 10).

A general introduction to the concepts common to many QMC methods has been given in Chap. 10. In this chapter, we focus on the issue of autocorrelations, which turns out to be of particular importance in the case of coupled fermion-boson models due to the different physical time scales involved, and the resulting problems in finding appropriate updating schemes. Quite disturbingly, some recent as well as early work seems to be unaware of the problem. To illustrate this point, we re-enact some specific QMC studies from the literature using the same methods, and demonstrate that statistical errors are severely underestimated if autocorrelations are neglected.

M. Hohenadler and T. C. Lang: *Autocorrelations in Quantum Monte Carlo Simulations of Electron-Phonon Models*, Lect. Notes Phys. **739**, 357–366 (2008)
DOI 10.1007/978-3-540-74686-7_11

This chapter is organized as follows. In Sect. 11.2, we introduce the model considered, and Sect. 11.3 gives a brief description of the algorithms used. Numerical evidence for the problem of autocorrelations is presented in Sect. 11.4, whereas their origin and a possible solution are the topic of Sect. 11.5. We end with our conclusions in Sect. 11.6.

11.2 Holstein Model

We consider the Holstein model which is defined by the Hamiltonian

$$H = -t \sum_{\langle i,j\rangle\sigma} c^\dagger_{i,\sigma} c_{j,\sigma} + \frac{\omega_0}{2} \sum_i (\widehat{p}_i^{\,2} + \widehat{x}_i^{\,2}) - \alpha \sum_{i,\sigma} \widehat{n}_{i,\sigma} \widehat{x}_i \,. \tag{11.1}$$

Here $c^\dagger_{i,\sigma}$ creates an electron with spin σ at site i, and $\widehat{n}_i = \sum_\sigma \widehat{n}_{i,\sigma}$ with $\widehat{n}_{i,\sigma} = c^\dagger_{i,\sigma} c_{i,\sigma}$. The phonon degrees of freedom at site i are described by the momentum $\widehat{p}_i$ and coordinate (displacement) $\widehat{x}_i$ of a harmonic oscillator. The model parameters are the nearest-neighbor hopping amplitude t, the Einstein phonon frequency ω_0 and the electron-phonon coupling α. We shall also refer to the spinless Holstein model, which can be obtained from (11.1) by dropping spin indices and sums over σ. We consider D-dimensional lattices with $V = N^D$ sites and periodic boundary conditions. A useful dimensionless coupling constant is $\lambda = \alpha^2/(\omega_0 W) = 2E_\mathrm{P}/W$, where $W = 4tD$ and E_P denote the free bandwidth and the polaron binding energy, respectively.

The Holstein model provides a framework to study numerous problems associated with electron-phonon interaction, such as polaron formation, superconductivity or charge-density-wave formation. Besides, more complicated models such as the Holstein-Hubbard model share the same structure of the phonon degrees of freedom and the electron-phonon interaction, so that the following discussion in principle applies to a wider range of problems.

11.3 Numerical Methods

To set the stage for the discussion of autocorrelations, we provide here a brief summary of the most important details of the different QMC algorithms employed. For details we refer the reader to [1, 2] and Chap. 10.

11.3.1 One-Electron Method

For the one-electron case (the polaron problem), we make use of the world-line method originally proposed in [3, 4]. Dividing the imaginary-time axis $[0, \beta]$ ($\beta = (k_\mathrm{B}T)^{-1}$ is the inverse temperature) into intervals of length $\Delta\tau = \beta/L \ll 1$

according to the Suzuki-Trotter approximation (see Chap. 10), the result for the fermionic[3] partition function reads

$$Z_{\mathrm{f},L} = \sum_{\{\boldsymbol{r}_\tau\}} w_\mathrm{f}(\{\boldsymbol{r}_\tau\})\,, \quad w_\mathrm{f}(\{\boldsymbol{r}_\tau\}) = \mathrm{e}^{\sum_{\tau,\tau'=1}^{L} F(\tau-\tau')\delta_{\boldsymbol{r}_\tau,\boldsymbol{r}_{\tau'}}} \prod_{\tau=1}^{L} I(\boldsymbol{r}_{\tau+1}-\boldsymbol{r}_\tau)\,, \tag{11.2}$$

with the fermionic weight w_f. The fermion world-lines, specified by a position vector $\boldsymbol{r}_\tau$ on each time slice,[4] are subject to periodic boundary conditions both in real space and imaginary time, and the sum in (11.2) is over all allowed configurations.

The retarded electron (self-)interaction due to electron-phonon coupling is described by the memory function

$$F(\tau) = \frac{\omega_0 \Delta\tau^3 \alpha^2}{4L} \sum_{\nu=0}^{L-1} \frac{\cos(2\pi\tau\nu/L)}{1-\cos(2\pi\nu/L)+(\omega_0\Delta\tau)^2/2}\,, \tag{11.3}$$

whereas electron hopping is manifest in the Fourier-transformed lattice propagator

$$I(\boldsymbol{r}) = \frac{1}{V}\sum_{\boldsymbol{k}} \cos(\boldsymbol{k}\cdot\boldsymbol{r})\,\mathrm{e}^{2\Delta\tau t\sum_{\zeta=1}^{D}\cos k_\zeta}\,. \tag{11.4}$$

The system described by the partition function (11.2) is characterized by an additional dimension (imaginary time), as well as by a complicated retarded (i.e., non-local in imaginary time) interaction. As first shown in [3], it may be simulated by means of Markov Chain MC in combination with the Metropolis algorithm [5]. The updating consists in choosing a random time slice $\tau_0 \in [1, L]$ and a random spatial component $\zeta_0 \in [1, D]$, and proposing a local change $r'_{\tau_0,\zeta_0} = r_{\tau_0,\zeta_0} \pm 1$, which is to be accepted with probability $\min[1, w_\mathrm{f}(\boldsymbol{r}'_\tau)/w_\mathrm{f}(\boldsymbol{r}_\tau)]$.

11.3.2 Many-Electron Method

A frequently used method for simulations of many-electron systems is the grand-canonical determinant QMC method [2], introduced for interacting fermions in Chap. 10. The corresponding grand-canonical Hamiltonian reads $H - \mu\sum_{i,\sigma}\widehat{n}_{i,\sigma}$, where μ denotes the chemical potential. For the Holstein model, the integration over the fermionic degrees of freedom can be done exactly, whereas for the Holstein-Hubbard model with electron-electron interaction it is done by means of MC sampling over Hubbard-Stratonovitch fields (see Chap. 10).

In the original approach of [2], the Trotter approximation to the partition function reads

[3] The bosonic part can be calculated exactly [4] and is therefore not considered.

[4] We use bold symbols to indicate the vector character of a quantity. The exact definition of the components should be clear from the context.

$$Z_L = \text{const.} \int \mathcal{D}\boldsymbol{x} \underbrace{\prod_{\sigma} \det\left[(1 + \prod_{\tau=1}^{L} \mathrm{e}^{-\Delta\tau K^{\sigma}} \mathrm{e}^{-\Delta\tau I^{\sigma}(\{\boldsymbol{x}_\tau\})}\right]}_{w_{\mathrm{f}}(\{\boldsymbol{x}_\tau\})} \underbrace{\mathrm{e}^{-\Delta\tau S_{\mathrm{b}}(\{\boldsymbol{x}_\tau\})}}_{w_{\mathrm{b}}(\{\boldsymbol{x}_\tau\})}, \tag{11.5}$$

with K^{σ}, I^{σ} denoting the matrix representations of the spin-σ component of the first respectively last term (including the minus signs) in Hamiltonian (11.1).

The bosonic action is given by

$$S_{\mathrm{b}}(\{\boldsymbol{x}_\tau\}) = \sum_{i=1}^{V} \sum_{\tau=1}^{L} \left[\frac{\omega_0}{2} x_{i,\tau}^2 + \frac{1}{2\omega_0 \Delta\tau^2} \left(x_{i,\tau} - x_{i,\tau+1}\right)^2 \right] = \sum_{i=1}^{L} \boldsymbol{x}_i^{\mathrm{T}} A\, \boldsymbol{x}_i \,. \tag{11.6}$$

Here the sampling is over all possible phonon configurations $\{\boldsymbol{x}_\tau\}$ of the bosonic degrees of freedom. In the simplest approach, we select a random time slice $\tau_0 \in [1, L]$ and a random lattice site $i_0 \in [1, V]$, and propose a modified phonon configuration $x'_{i_0,\tau_0} = x_{i_0,\tau_0} \pm \delta x$. The latter is then accepted with probability $\min[1, w_{\mathrm{f}}(\{\boldsymbol{x}'_\tau\}) w_{\mathrm{b}}(\{\boldsymbol{x}'_\tau\}) / w_{\mathrm{f}}(\{\boldsymbol{x}_\tau\}) w_{\mathrm{b}}(\{\boldsymbol{x}_\tau\})]$. The change δx is determined by requiring a reasonable acceptance rate. An improved (global) updating scheme will be discussed below.

11.4 Problem of Autocorrelations

We now come to a discussion of autocorrelations, which are analyzed using the binning and Jackknife methods introduced in Chap. 4. As shown in there, the integrated autocorrelation time $\tau_{\mathcal{O},\mathrm{int}}$ associated with an observable $\mathcal{O}$ can be estimated by plotting the statistical error as obtained from a binning/Jackknife analysis as a function of binsize k, and deducing the binsize required for "saturation". The increase of the error with increasing k demonstrates the fact that unjustified neglect of autocorrelations leads to an underestimation of errors and hence to incorrect results. Explicitly, the statistical error $\Delta\mathcal{O}$ for a given number of (correlated) measurements N_{meas} increases with $\tau_{\mathcal{O},\mathrm{int}}$ as $(\Delta\mathcal{O})^2 \propto 2\tau_{\mathcal{O},\mathrm{int}}/N_{\mathrm{meas}}$.

11.4.1 One-Electron Case

As a specific case, we consider world-line simulations of the Holstein polaron, i.e., the Hamiltonian (11.1) with a single electron. This problem has first been studied by means of QMC in [3]. The same method has also been used in [6] as well as in [7], and its generalizations represent a versatile tool for studies of more general systems with one or two fermions. In [3, 6], the authors skipped L (the number of time slices) steps between successive measurements.

We take $\lambda = 1$, close to the critical coupling where the small-polaron crossover occurs in the adiabatic regime [8], leading to the occurrence of critical slowing down

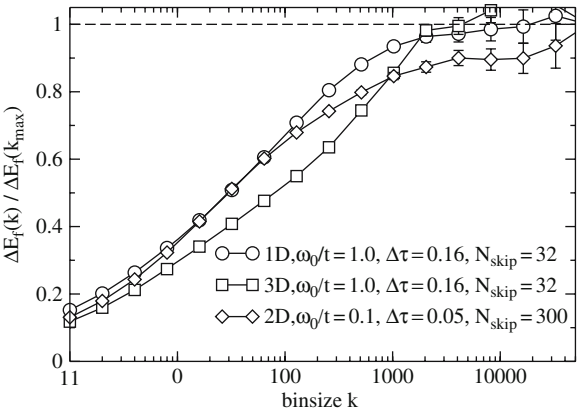

Fig. 11.1. Statistical error of the fermionic total energy E_f as a function of binsize k, normalized to the result for the maximum binsize, obtained with the world-line method [4]. Results are for the Holstein model with one electron, $N = 32$ and $\lambda = 1$

for $\omega_0/t \lesssim 1$ [7]. To compare with [4], we choose the same parameters $\beta t = 5$, $L = 32$, $N = 32$ and $\omega_0/t = 1$.

In Fig. 11.1, we show results for the statistical error of the fermionic contribution to the total energy[5] as obtained from a binning analysis with variable binsize k. The uncertainty of the binning error increases with decreasing binsize, leading to fluctuations. Note the logarithmic scale on the abscissa.

Skipping $N_\mathrm{skip} = L = 32$ steps between measurements, we find for the 1D case that the statistical error increases roughly by a factor of 7, i.e., it is substantially larger than the estimate obtained from binning with $k = 1$, which corresponds to the usual procedure to calculate statistical errors from uncorrelated data.

The situation is slightly worse in three dimensions, with the real error being again about an order of magnitude larger. This may be related to the local updating, as the relative difference between two entire successive world-line configurations is smaller in higher dimensions if only a single coordinate r_{τ_0,ζ_0} is changed.

Finally, we also consider the more demanding 2D case of low temperature $\beta t = 15$ and small phonon frequency $\omega_0/t = 0.1$, which has been studied using the same method in [6, 7]. As discussed below, the smaller values of ω_0 and $\Delta\tau$ give rise to substantially longer autocorrelation times. Indeed, despite the larger number of skipped steps $N_\mathrm{skip} = L = 300$, convergence of the statistical error is slower as a function of k.

An alternative algorithm free of autocorrelations, which can also be applied to the many-electron case, has been proposed in [9] and will be discussed in Sect. 11.5.

11.4.2 Many-Electron Case

It is important to point out that the occurrence of long autocorrelation times is not restricted to the one-electron case. The problem is at least as serious for the

[5] Autocorrelation times are similar for other observables.

two-electron model [7], and accurate simulations in the many-electron case turn out to be unfeasible in many cases [10] due to autocorrelations times exceeding 10^4 MC steps.

To illustrate this point, we consider two parameter sets for the Holstein model at half filling (one electron per lattice site), representative of the work in [11] and [12]. We use the finite-temperature determinant QMC method, although the results of [11] have been obtained using the projector method (see Chap. 10; autocorrelation times are usually comparable). Owing to the substantially larger computational effort as compared to one-electron calculations, we were not able to obtain converged results. Therefore, and to compare different parameters, we show in Fig. 11.2 the statistical error of the bosonic energy $E_\mathrm{b} = (\omega_0/2)\langle\sum_i(\widehat{p}_i^2 + \widehat{x}_i^2)\rangle$, normalized to the error for binsize $k = 1$. The definition of λ in terms of the coupling constant g used in [11, 12] reads $\lambda = 2g^2/(\omega_0 W)$, and we have used $N_\mathrm{skip} = 1$.

The strong increase of statistical errors as a function of binsize in Fig. 11.2 illustrates the substantial autocorrelations in such simulations. No saturation can be seen in our data even for the largest binsize $k > 10^4$ shown (cf Fig. 11.1) and, in contrast to the world-line method of Sect. 11.3, skipping thousands of steps is usually not practicable in the many-electron case. In our opinion, this suggests that reliable results for the Holstein model in the many-electron case are extremely challenging to obtain using the determinant QMC method, and the situation becomes even worse for $\omega_0/t < 1$. Similar conclusions can be drawn about the spinless Holstein model, models with phonon modes of different symmetry [10], as well as Holstein-Hubbard models with local and/or non-local Coulomb interaction [13].

Despite these difficulties, some early work [12] as well as more recent papers, e.g., [11, 14], seem to be unaware of this problem. This issue becomes even more critical if dynamical quantities such as the one-electron spectral function are

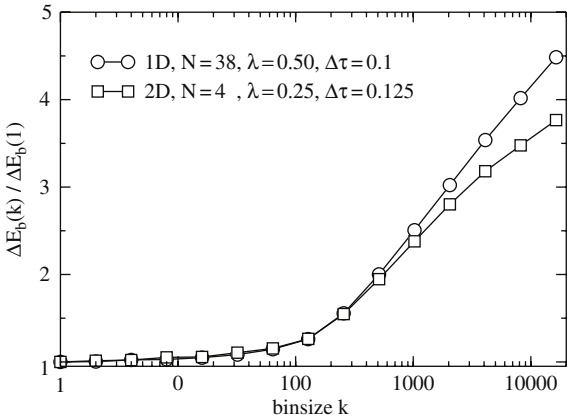

Fig. 11.2. Statistical error of the bosonic energy E_b as a function of binsize k, normalized to the result for $k = 1$, obtained with the determinant QMC method [2]. Results are for the Holstein model at half filling $n = 1$, $\beta t = 10$ and $\omega_0/t = 1$. Errorbars are not shown

calculated. The reason lies in the necessity to perform an analytical continuation to real frequencies, which turns out to be an extremely ill-conditioned problem (see Chap. 12) whose solution – obtained for example by the Maximum Entropy method [15, 16] – depends crucially on the statistical noise of the input data (the imaginary-time Green function). Any underestimation of errors, or the neglect of significant autocorrelations between measurements on different time slices can lead to incorrect results. Furthermore, meaningful statistical errors for dynamical properties are difficult to obtain, and are often not reported at all.

11.5 Origin of Autocorrelations and Principal Components

To understand the problem and to find solutions, it is instructive to look at the physical origin of autocorrelations in more detail [9]. To this end, let us consider the non-interacting limit ($t = \alpha = 0$), in which the partition function $Z_L \sim \int \mathcal{D}x\, \mathrm{e}^{-\Delta\tau S_\mathrm{b}}$. As discussed in [17], the difficulties encountered in QMC simulations, even for the simple case of a single ($N = 1$) quantum-mechanical harmonic oscillator, result from the large condition number (the ratio of largest to smallest eigenvalue) of the matrix A in the bosonic action S_b (11.6). For $\Delta\tau \ll 1$, this number scales as $(\omega_0\Delta\tau)^{-2}$ [17], causing autocorrelation times to grow quadratically with decreasing phonon frequency or increasing number of Trotter slices L. This is very unfortunate, as small phonon frequencies are frequently encountered in materials of interest, and small values of $\Delta\tau$ are desirable to control the Trotter error.

The physical reason for these correlations becomes obvious if we look at the free bosonic action (11.6), which is proportional to the energy of a given phonon configuration. The first term of S_b corresponds to the kinetic energy of the oscillators, and the second term describes a coupling in imaginary time – a pure quantum-mechanical effect. Due to this interaction, a large change of a single phonon degree of freedom, x_{i_0,τ_0} say, is very unlikely to be accepted due to the associated large energy change $\sim (\omega_0\Delta\tau)^{-1}$. However, using only small changes Δx, successive phonon configurations will be highly correlated. This behavior carries over to the interacting case with one or many electrons, as well as to more general models.

The situation is not completely obvious for the world-line algorithm, because the phonon degrees of freedom are integrated out analytically. However, the retarded self-interaction entering simulations in terms of $F(\tau)$ (11.3) gives rise to the same problem. Moreover, for large α (strong coupling), electronic hopping becomes very unlikely ($F(\tau) \sim \alpha^2$), causing the acceptance rate to approach zero and thus again giving rise to autocorrelations.[6] The situation is expected to be slightly better for the continuous-time variant of the algorithm [18] because hopping events may occur at arbitrary points in imaginary time.

[6] In the world-line algorithm, the discrete step size used for updates cannot be reduced below one lattice constant.

We now discuss a solution for the problem of autocorrelations in simulations of certain Holstein-type models. It is based on a transformation of the bosonic action to a so-called principal-component representation [9], which is obtained by writing

$$S_{\mathrm{b}} = \sum_{i=1}^{V} \boldsymbol{x}_i^{\mathrm{T}} A\, \boldsymbol{x}_i = \sum_{i=1}^{V} \boldsymbol{x}_i^{\mathrm{T}} A^{1/2} A^{1/2}\, \boldsymbol{x}_i = \sum_{i=1}^{V} \boldsymbol{\xi}_i^{\mathrm{T}} \cdot \boldsymbol{\xi}_i\,, \quad \boldsymbol{\xi}_i = A^{1/2} \boldsymbol{x}_i\,, \quad (11.7)$$

with the aforementioned $L \times L$ matrix A, and the principal components $\boldsymbol{\xi}$, in terms of which S_{b} becomes diagonal. Using this representation, the bosonic weight reduces to a Gaussian distribution, $w_{\mathrm{b}} = \exp(-\Delta\tau \sum_i \boldsymbol{\xi}_i^{\mathrm{T}} \cdot \boldsymbol{\xi}_i)$. For $\alpha = 0$, sampling can be done exactly in terms of the new variables $\xi_{i,\tau}$ using the Box-Muller method [19].

To further illustrate the origin of autocorrelations, as well as the transformation to principal components, we show in Fig. 11.3(a) a schematic representation of the distribution of values for a pair (p, p') of two phonon momenta (shaded area). The elongated shape originates from the strong correlations mediated by S_{b}, and requires a transition $A \to B$ between two points in phase space to be performed in many small steps, leading in turn to long autocorrelation times.

In contrast, the axes of the principal components ξ, ξ' in Fig. 11.3(b) lie along the axes of the ellipse, and a single MC update of ξ' is sufficient to get from A to B. Although we have sketched the more general case, the distribution after the exact transformation (11.7) – under which w_{b} becomes a Gaussian – is actually circular in the new variables ξ, ξ' (dashed line in Fig. 11.3(b)).

Whereas exact sampling without autocorrelations is straightforward in the non-interacting case $\alpha = 0$, the dependence of w_{f} on the phonon coordinates $x_{i,\tau}$ for $\alpha > 0$ does not permit a simple separation of bosonic and fermionic contributions in the updating process. Therefore, it has been proposed [9] to base the QMC algorithm on the Lang-Firsov transformed Hamiltonian, which has no explicit coupling of x to electronic degrees of freedom. To this end, it is advantageous to sample the phonon momenta p instead of x, as the former depend only weakly on the electronic degrees of freedom [9], which enables us to treat the fermionic weight w_{f}

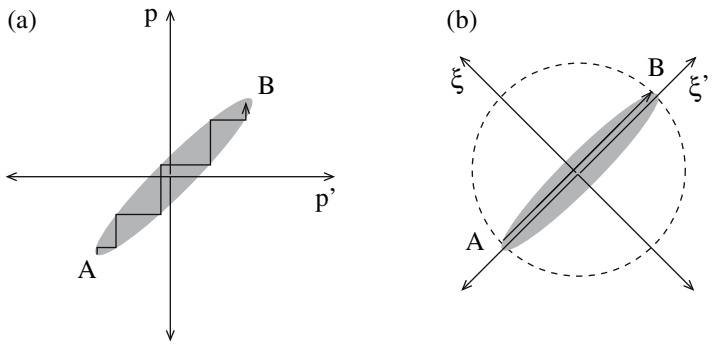

Fig. 11.3. Schematic illustration of the transformation from phonon momenta p, p' to principal components ξ, ξ' (see text)

as a part of the observables, and renders the MC sampling exact and rejection-free (every new configuration is accepted). Consequently, we avoid a warm-up phase, autocorrelations and the computationally expensive evaluation of w_{f} in the updating process.

The method outlined here has been successfully applied to the polaron [9, 20], bipolaron [21], and the (spinless) many-polaron problem [22]. Unfortunately, attempts to generalize this approach to the Holstein-Hubbard model, or the spinful Holstein model, have not been successful [13]. Although the Lang-Firsov transformation improves the sampling of phonon configurations via principal components, the complex phase in the transformed hopping term [9] induces a severe sign problem [13, 22]. Despite encouraging acceptance rates, this global updating scheme does not permit reliable statements concerning a possible decrease of autocorrelation times.

11.6 Conclusions

By revisiting several QMC studies of Holstein models carried out in the past we have illustrated the severe problem of autocorrelations in simulations of electron-phonon models, in accordance with [10]. In particular, we have shown that statistical errors can be underestimated by orders of magnitude if autocorrelations are neglected. This is particularly dangerous when calculating dynamic properties using, e.g., Maximum Entropy methods, where meaningful errorbars can usually not be obtained, introducing substantial uncertainties into the results. Long autocorrelation times can also lead to critical slowing down as well as non-ergodic sampling during finite-time MC runs – both phenomena being additional sources for underestimated statistical errors – thereby also affecting the expectation values of observables.

Similar to the infamous minus-sign problem (see Chap. 10), autocorrelations in QMC simulations seem to result from the fact that one is dealing with an ill-conditioned physical problem. As a consequence, their appearance is not restricted to the Holstein-type models considered here (see Chap. 10), or the particular QMC methods employed. Besides, autocorrelations even occur in simulations of classical systems (Chap. 4), although the problem is usually not as substantial as for coupled fermion-boson systems. This general observation strongly suggests that great care has to be taken when performing any MC simulations in order to avoid incorrect results.

Significant advances in terms of efficiency and applicability can be achieved by constructing a physically motivated global updating scheme. One such possibility has been presented here in terms of a transformation to principal components. However, a general solution to overcome the problem of autocorrelations in simulations of electron-phonon models is not yet known.

Acknowledgements

MH acknowledges financial support by the Austrian Science Fund (FWF) through the Erwin-Schrödinger Grant No J2583. We thank Pavel Kornilovitch for useful discussion.

References

1. H. de Raedt, A. Lagendijk, Phys. Rep. **127**, 233 (1985) 358
2. R. Blankenbecler, D.J. Scalapino, R.L. Sugar, Phys. Rev. D **24**, 2278 (1981) 358, 359, 362
3. H. De Raedt, A. Lagendijk, Phys. Rev. Lett. **49**, 1522 (1982) 358, 359, 360
4. H. De Raedt, A. Lagendijk, Phys. Rev. B **27**, 6097 (1983) 358, 359, 361
5. N. Metropolis, A. Rosenbluth, A. Teller, E. Teller, J. Chem. Phys. **21**, 1087 (1953) 359
6. P.E. Kornilovitch, J. Phys.: Condens. Matter **9**, 10675 (1997) 360, 361
7. M. Hohenadler, H. Fehske, J. Phys.: Condens. Matter **19**, 255210 (2007) 360, 361, 362
8. H. Fehske, A. Alvermann, M. Hohenadler, G. Wellein, in *Polarons in Bulk Materials and Systems with Reduced Dimensionality*, ed. by G. Iadonisi, J. Ranninger, G. De Filippis (IOS Press, Amsterdam, Oxford, Tokio, Washington DC, 2006), Proc. Int. School of Physics "Enrico Fermi", Course CLXI, pp. 285–296 360
9. M. Hohenadler, H.G. Evertz, W. von der Linden, Phys. Rev. B **69**, 024301 (2004) 361, 363, 364, 365
10. D. Eckert, Phononen im Hubbard Modell. Master's thesis, University of Würzburg (1997) 362, 365
11. K. Tam, S. Tsai, D.K. Campbell, A.H. Castro Neto, Phys. Rev. B **75**, 161103 (2007) 362
12. P. Niyaz, J.E. Gubernatis, R.T. Scalettar, C.Y. Fong, Phys. Rev. B **48**, 16 011 (1993) 362
13. T.C. Lang, Dynamics and charge order in a quarter filled ladder coupled to the lattice. Master's thesis, TU Graz (2005) 362, 365
14. C.E. Creffield, G. Sangiovanni, M. Capone, Eur. Phys. J. B **44**, 175 (2005) 362
15. W. von der Linden, Phys. Rep. **220**, 53 (1992) 363
16. M. Jarrell, J.E. Gubernatis, Phys. Rep. **269**, 133 (1996) 363
17. G.G. Batrouni, R.T. Scalettar, in *Quantum Monte Carlo Methods in Physics and Chemistry*, ed. by M.P. Nightingale, C.J. Umrigar (Kluwer Academic Publishers, Dordrecht, 1998), p. 65 363
18. P.E. Kornilovitch, Phys. Rev. Lett. **81**, 5382 (1998) 363
19. G.E.P. Box, M.E. Muller, Ann. Math. Stat. **29**, 610 (1958) 364
20. M. Hohenadler, H.G. Evertz, W. von der Linden, phys. stat. sol. (b) **242**, 1406 (2005) 365
21. M. Hohenadler, W. von der Linden, Phys. Rev. B **71**, 184309 (2005) 365
22. M. Hohenadler, D. Neuber, W. von der Linden, G. Wellein, J. Loos, H. Fehske, Phys. Rev. B **71**, 245111 (2005) 365